# General Disclaimer

## One or more of the Following Statements may affect this Document

- This document has been reproduced from the best copy furnished by the organizational source. It is being released in the interest of making available as much information as possible.

- This document may contain data, which exceeds the sheet parameters. It was furnished in this condition by the organizational source and is the best copy available.

- This document may contain tone-on-tone or color graphs, charts and/or pictures, which have been reproduced in black and white.

- This document is paginated as submitted by the original source.

- Portions of this document are not fully legible due to the historical nature of some of the material. However, it is the best reproduction available from the original submission.

Produced by the NASA Center for Aerospace Information (CASI)

# NASA TECHNICAL MEMORANDUM

## NASA TM-78945

NASA TM-78945

# EFFECTS OF PRESSURE AND TEMPERATURE
# ON HOT PRESSING A SIALON

by Hun C. Yeh and William J. Waters
Lewis Research Center
Cleveland, Ohio 44135

# EFFECTS OF PRESSURE AND TEMPERATURE ON HOT PRESSING A SIALON

by Hun C. Yeh and William J. Waters

Lewis Research Center
National Aeronautics and Space Administration
Cleveland, Ohio

## INTRODUCTION

Sialons are ceramics composed of elements silicon (Si), aluminum (Al), oxygen (O) and nitrogen (N). It was suggested that fully dense single phase sialons might be more attractive than $Si_3N_4$ for high temperature structural applications, especially from an ease of fabrication point of view.[1,2] In addition, the strength of a truly single phase $\beta'$ ($\beta'$ is formed by dissolving various amounts of AlN and $Al_2O_3$ into the structure of $\beta-Si_3N_4$) body should not degenerate as significantly at high temperature as does hot-pressed $Si_3N_4$ which usually contains a lower melting second phase.

Jack and Wilson claimed that they were able to pressureless sinter mixes of $Al_2O_3$ and $Si_3N_4$ powders to maximum density $\beta'$ bodies.[1] However, the moderate room temperature bend strength reported by them would suggest the presence of additional phase(s) and/or pores in the sintered body. They did not report any high temperature bend strength results. Arrol reported a fully dense hot-pressed $\beta'$ body having bend strength of 825 MPa (120 Ksi) at as high as $1200^\circ C$.[2] The best $\beta'$ body produced by pressureless sintering reported in his paper was only 91 percent dense with a room temperature bend strength of 330 MPa (48 Ksi).

Subsequently, many attempts were made by other investigators to pressureless sinter single phase $\beta'$ bodies without success.[3,4,5] Layden successfully made $\beta'$ directly into powder form but then found that this powder did not sinter. He concluded that a certain amount of liquid phase was necessary to accomplish pressureless sintering of dense $\beta'$ bodies.[5] Consequently, a

transient liquid phase (TLP) process was developed.[6] The resulting $\beta'$ body still contained a very minor amount of other phase(s) as reflected by the low room temperature bend strength and the deterioration of strength at higher temperatures. In view of the difficulties encountered in the pressureless sintering process, hot-pressing, although usually more expensive, should still be investigated further as an alternative process for producing dense sialon materials with minimal amounts of second phase.

Almost all earlier hot-pressing studies of Si-Al-O-N ceramics reported employed a pressure 27.5 MPa (4 Ksi) or higher and a temperature $1700^{\circ}$C or higher. Two recent papers by one of the authors of this paper dealt with the hot-pressing behavior of 60 m/o $Al_2O_3$-40 m/o $Si_3N_4$ powder compacts[7,8] concentrating on temperature effects, microstructure, and phase transformations. The present paper is a continuation of the above work, investigating the effect of pressure in combination with temperature.

The objective of this investigation was to determine the combined effects of temperature and pressure on the resulting density of sialon.

The composition studied (60 m/o $Al_2O_3$-40 m/o $Si_3N_4$) has now been established to lie in a phase region ($\beta'$ and X) in the $Si_3N_4$, $Al_2O_3$, AlN and $SiO_2$ "equilibrium" diagram rather than in the homogeneity region of $\beta'$ phase[9]; therefore, it may not have as attractive applications as it was once believed to have. However, the results of this investigation may provide more basic understanding about the as yet not fully explored family of nitrogen ceramics with respect to processing and phase equilibria.

The pressure and temperature ranges studied in this paper were 3.5 MPa (0.5 Ksi) to 27.5 MPa (4 Ksi) and $1550^{\circ}$ to $1750^{\circ}$C.

## EXPERIMENTAL PROCEDURES

### Materials

Starting materials consisted of commercially produced powders of $\alpha$-$Si_3N_4$ and $\gamma$-$Al_2O_3$. The supplier of the $Si_3N_4$ powder reported it to be 94 percent $\alpha$ phase and 6 percent $\beta$ phase. The total impurity of the $Si_3N_4$ was reported as 1.3? wt.%. The impurities were reported to be 0.92 percent 0, 0.22 percent C, <0.01 percent Ca, <0.12 percent Al, and <0.05 percent Fe. The $Al_2O_3$ powder was reported to have a metallic impurity level of less than 0.1 percent. Nonmetallic impurities were not reported. The $Al_2O_3$ powder was reported to be essentially 100 percent $\gamma$ phase.

The morphology and size range of the as received powders were determined by transmission electron microscopy. The $Si_3N_4$ powder consisted of both fibrous and flakelike crystallites. The fibres had diameters ranging from 0.04 to 0.3 $\mu$m and random lengths. Platelet type flakes ranged from 0.02 to 1.0 $\mu$m in maximum dimension with random thicknesses, orders of magnitude thinner than the maximum dimension. The $Al_2O_3$ powder was spherical and ranged in size from 0.005 to 0.09 $\mu$m with a predominant size range of from 0.01 to 0.02 $\mu$m.

### Apparatus and Procedure

The powders used in this investigation were mixed in the mol ratio of 60 $Al_2O_3$/40 $Si_3N_4$. This resulted in a powder mixture of 52.2 wt.% $Al_2O_3$ and 47.8 wt.% $Si_3N_4$. Charges of mixed powder of 100 gm. were processed in the following manner: The as received powders were weighed and charged into a 0.1M diameter steel attritor. Added to the attritor were 2200 gm. of 3mm diameter steel balls together with about 400 ml (380 ml heptane, 20 ml of grain alcohol) of liquid carrier. The attritor was run in air at 350

rpm. for 2 hours.

Blended powders were removed from the attritor and dried in two steps. Preliminary drying was done in air and final drying was done in vacuum. Total drying time was 24 hours and resulted in maximum moisture removal. Based on previous studies,[7] estimated pickup of oxygen was 1.6 to 2.5 wt.% and of iron was 0.4 to 0.8 wt.%.

Transmission electron microscopy examination of the processed powders revealed that the spherical $Al_2O_3$ and flakelike $Si_3N_4$ particles were unchanged in morphology while the fibrous $Si_3N_4$ had been broken into smaller lengths.

Hot pressing of the blended powders was accomplished in a noncommercial induction heated vacuum hot press facility, powered by a 9600Hz, 50 KW motor generator. A graphite susceptor 16.5 cm O.D., X 15.5 cm I.D. x 20 cm long was used to evenly heat the graphite die assembly which measured 15 cm diameter by 15 cm long. Temperatures were monitored with a W-Re thermocouple inserted in the die body, adjacent to the powder cavity. Previous runs in this unit had indicated good agreement between optical and thermocouple readings.

Blended powder (20 to 40 gm) was precompacted by pressing at room temperature and 27.5 MPa (4 Ksi) in the graphite die assembly. The powder was contained in the die cavity (5.7 cm x 1.25 cm). The die cavity was lined with graphite inserts (.1 cm thick) that had been coated with boron nitride. The boron nitride had been painted on as a water suspension (90 percent distilled water, 10 percent BN powder) and air dried with a heat lamp. Inserts coated with BN acted as a reaction barrier between the powder compact and the graphite die body.

The graphite die containing the cold pressed powder was loaded into the hot press and a specified pressure was applied under vacuum. After 5 minutes of vacuum pumpdown, a flowing helium atmosphere was introduced into the system and the heating cycle started. The pressure on the powder die was maintained

by a self-adjusting control valve during the heating and hold cycle of the hot pressing operation. Holding time (at temperature) was generally about 2 hours. Hold temperatures ranged from $1350^{\circ}$ to $1700^{\circ}$C. Pressure ranged from 15 to 27.5 MPa (.5 to 4 Ksi). Figure 1 shows the hot-pressing conditions chosen for investigation. Single tests were run for all conditions. Temperature and ram travel were continuously recorded. Temperature was monitored by a digital millvolt meter. Temperature control was maintained by the test facility operator who controlled the power imput. Temperatures were generally maintained at $\sim 20^{\circ}$C during the 2 hour hold portion of the hot press cycle. Heating cycles were not automatically controlled so the rate of temperature increase varied to some degree. A typical heating rate curve is shown in Figure 2.

To monitor the compacting behavior of the powder compact during both the heating and the hold cycles of the hot pressing operation, ram travel was measured with an LVDT (variable resistance) extensometer and recorded. A typical ram travel plot is also shown in Figure 2.

Transmission electron microscopy specimens were prepared from the hot-pressed specimens using a commercial ion beam thinning apparatus and were examined on an electron microscope. X-ray diffraction patterns were obtained on powders ground from the center portion of each hot-pressed specimen.

RESULTS AND DISCUSSION

Density and Microstructure

All density values were measured after a 2-hour hold at the specified temperature and pressure. For the purpose of discussion and comparison, the measured density results were also expressed in percent of the theoretical density, $\rho_R$ of $\beta$-$Si_3N_4$ (3.18 gm/cc). Figure 3 shows the effect of hot pressing pressure on the density of the specimen for the four different holding

temperatures chosen for study. For the lowest temperature investigated, $1550^{\circ}$C, the density increased drastically as the pressure was increased from 3.5 to 14 MPa (0.5 to 2 Ksi); essentially, no noticeable density increase was observed from 14 to 21 MPa (2 Ksi to 3 Ksi); and then another drastic increase in density was observed when the pressure was raised to 27.5 MPa (4 Ksi).

The initial increase in density at $1550^{\circ}$C in the pressure range 3.5 to 14 MPa (0.5 to 2 Ksi) was attributed to particle rearrangement and sliding mechanisms. This resulted in a partially sintered structure containing many voids as shown by the TEM micrograph in Fig. 4a. The grains are predominantly equiaxed ranging from 0.3 to 1 μm in size. Very few, if any, of the starting fine spherical $\gamma$-$Al_2O_3$ particles ($\sim$ 0.02 μm) were found in the micrograph (Fig. 4a). X-ray diffraction data of samples pressed at $1550^{\circ}$C showed a significant amount of $\alpha$-$Al_2O_3$ but no $\gamma$-$Al_2O_3$. Thus, it was apparent that the starting $\gamma$-$Al_2O_3$ had transformed to $\alpha$-$Al_2O_3$ and part of the equiaxed grains in the micrograph are $\alpha$-$Al_2O_3$. Solid state reaction had already taken place between particles (grains) as evident by the good bonds formed between grains; this is more clearly shown in Fig. 4b. Striated grains typical of X-phase[10] were not observed in the micrographs and this was in agreement with the X-ray results to be presented.

The marked increase in density when 27.5 MPa (4 KSI) was used can be explained by plastic deformation that occurred in the sample. This was evidenced by dislocation lines and networks and pore-free microstructure found in figure 5. X-ray results to be presented will reveal more information on the densification mechanism.

For the $1600^{\circ}$C runs, the density increased drastically to nearly full density when the pressure was increased from 7 to 14 MPa (1 to 2 KSI) and then no further increase in density was observed when pressure was increased from 14 to 27.5 MPa (2 to 4 KSI).

For 1700°C runs, a full density body was obtained at as low as 7 MPa (1 Ksi) while a pressure of only 3.5 MPa (0.5 Ksi) was sufficient to produce a fully density body at 1750°C. Transmission electron microscopy examination of the fully dense specimens made at 1600°C, 1700°C and 1750°C did not show any significant difference from the microstructure shown in figure 5.

The minimum pressure required to produce a full density body decreased as the temperature was increased. It is interesting that a pressure of 7 MPa (1 Ksi) was sufficient to produce a full density body at 1700°C as compared with the general practice of using 27.5 MPa (4 Ksi) or higher.

The effect of temperature on density at a given level of applied pressure can be more clearly observed in Fig. 6 where the measured density is plotted against temperature.

Iso-density contours at 5 percent $\rho_R$ interval as shown in Fig. 7 can also be constructed based on the curves in Fig. 6. The shaded area outlines the full density region which is 98% of the theoretical density of $^\beta$ $Si_3N_4$. Such a map could be used to define the broad range of temperature and pressure conditions to obtain a specific density. This then may assist in predicting microstructures of sialon materials.

X-ray Phase Analysis

A semiquantitive method was used to express the trend of relative change of phases in samples. Figures 8a through 8c are such plots showing the variation in phase content as a function of pressure for 1550°, 1600°, and 1700°C runs, respectively. These results support and supplement the observation presented in the previous section.

For the 1550°C runs, one of the most significant features was the appearance of a trace amount of X-phase at 17 MPa (2.5 Ksi) and the increased levels of X-phase at 21 and 27.5 MPa (3 Ksi and 4 Ksi). The much higher density value

of the 27.5 MPa (4 Ksi) sample as compared with the 21 MPa (3 Ksi) sample (fig. 3) could reflect possible plastic deformation in the material as indicated by the dislocations evident in Fig. 5. The continued reduction in $\alpha$-$Si_3N_4$ phase as the pressure was increased might also play a role in the densification process. A significant amount of $\alpha$-$Al_2O_3$ was present in all samples but no $\gamma$-$Al_2O_3$ was detectable. Our earlier work[7] showed that $\gamma$-$Al_2O_3$ began transforming to $\alpha$-$Al_2O_3$ below 1200°C and had completely transformed at 1300°C.

It is interesting to note in comparing Figs. 8(a) and (b) that with an increase of 50°C, from 1550°C to 1600°C, all $\alpha$-$Si_3N_4$ was eliminated even for the 7 MPa (1 Ksi) sample--the lowest pressure investigated at 1600°C; also, the X-phase was present at 7 MPa ( 1 KSI) and had a higher relative X-ray peak intensity than that of $\alpha$-$Al_2O_3$ out to 27.5 MPa (4 KSI). As the pressure was increased to 27.5 MPa (4 Ksi), $\beta'$ phase became predominant and only trace amounts of $\alpha$-$Al_2O_3$ and X-phase were detected. This probably was the equilibrium state of the specimen at 1600°C.

Figure 9 is a behavioral or quasi phase equilibrium diagram for the sialon system[9]. The composition chosen for study in this paper is the 60 m/o $Al_2O_3$ - 40 m/o $Si_3N_4$ composition and is so marked on the figure. This composition is located in the ( $\beta'$+X) region. Figure 9 may be used as a guide to understand the reaction between $Al_2O_3$ and $Si_3N_4$ particles in the powder compact under hot-pressing. As the reaction progresses toward the equilibrium state ( $\beta'$ and X-phase), $Al_2O_3$ should diminish as more $\beta'$ and X-phases are formed. Eventually, $Al_2O_3$ disappears and X-phase also reduces in amount relative to the increased amount of $\beta'$ formed. The above trend was observed for the 1600°C runs as pressure increases (Fig. 8b). With increasing pressure, the continued change in phase content toward "more equilibrium state" suggested that pressure enhances the

reaction.

For the 1700°C runs, Fig. 8c, $Al_2O_4$ did not appear even in the sample hot-pressed at only 3.5 MPa (0.5 Ksi). The decline in X-phase with increasing pressure could be due to further interaction between X and $\beta'$ to reach an equilibrium condition.

Figure 10 shows the consistent increase in unit cell size of the $\beta'$ phase as a function of pressure for all temperatures investigated using C-axis as an indicator. The systematic increase in C-axis as pressure increases is further evidence that pressure enhances the phase equilibria reaction. It is also of interest to note the slower but continuous increase in "C" for 1600°C runs beyond 14 MPa (2 Ksi) and the 1700°C runs beyond 7 MPa (1 Ksi). Both conditions (1600°C - 14 MPa, 1700°C - 7 MPa) correspond to the first full density samples of their respective temperature series of runs.

CONCLUDING REMARKS

1. Fully dense sialon bodies (+98% $\rho_R$) can be produced by hot-pressing at a pressure much lower than the general practice in the field. For example, only 7 MPa (1 Ksi) was sufficient at 1700°C and 14 MPa (2 Ksi) at 1600°C as compared with 27.5 MPa (4 Ksi) at the lower temperature of 1550°C.

2. Increased pressure enchances the phase equilibrium reaction.

3. Iso-density contour can be constructured for the sialon composition chosen for study. This diagram has potential to help design desired micro - structures.

4. The densification of the sialon studied was very sensitive to the phase changes (solids or liquids) taking place in the sample during hot pressing.

5. Microstructures of samples exceeding 98% theoretical density offer evidence that plastic deformation has contributed to densification.

REFERENCES

1. K. H. Jack, and W. I. Wilson, "Ceramics Based on the Si-Al-O-N and Related Systems," Nature (London), Phys. Sci., 238 (80), 28-29 (1972).

2. W. J. Arrol, Chapt. 34 in Ceramics for High-Performance Applications. Edited by J. J. Burke, Chesnut Hill, Mass., Brook Hill Publ. Co., 1974, pp. 729-738.

3. W. B. Crandall, A. Z. Hed and L. E. Shipley, "Preparation and Evaluation of Sialon," IIT Research Inst., Air Force Aeronautical Research Lab. TR-74-0099, June 1974.

4. F. F. Lange, "Fabrication and Properties of Silicon Compounds - Task 1. Fabrication Microstructure and Selected Properties of Sialon Compositions,' Westinghouse Research Labs, February 1974.

5. G. K. Layden, "Process Development for Pressureless Sintering of Sialon Ceramic Components," United Technologies Corp., UTRC/R75-912072-4, February 1976.

6. G. K. Layden, "Pressureless Sintering of Sialon Gas Turbine Components," United Technologies Corp., UTRC/R77-912532-4, February 1977.

7. H. C. Yeh, and W. A. Sanders, and J. L. Fiyalko Luttner, "Pressure Sintering of Sialon," Am. Ceram. Soc. Bull., 56 (2) 189-193 (1977).

8. H. C. Yeh, "Microstructure of Hot-Pressed $Al_2O_3$-$Si_3N_4$ Mixtures as a Function of Holding Temperature," in Ceramic Microstructures '76, Edited by R. M. Fulrath and J. A. Pask, Boulder, Colo., Westview Press, 1977, pp. 444-455.

9. K. H. Jack, "Sialons and Related Nitrogen Ceramics," J. Mater. Sci., 11 1135-1158 (1976).

10. P. Drew, and M. H. Lewis, "The Microstructures of Silicon Nitride/ Alumina Ceramics," J. Mater. Sci., 9 1833-38 (1974).
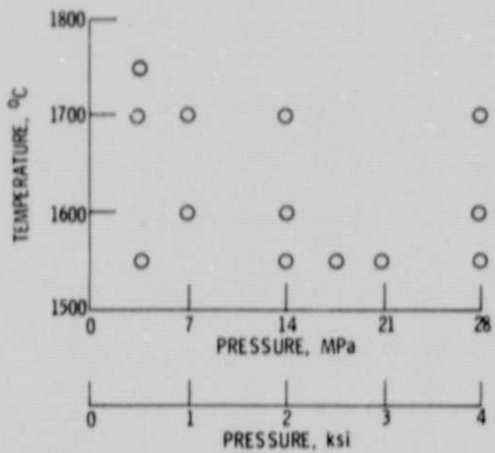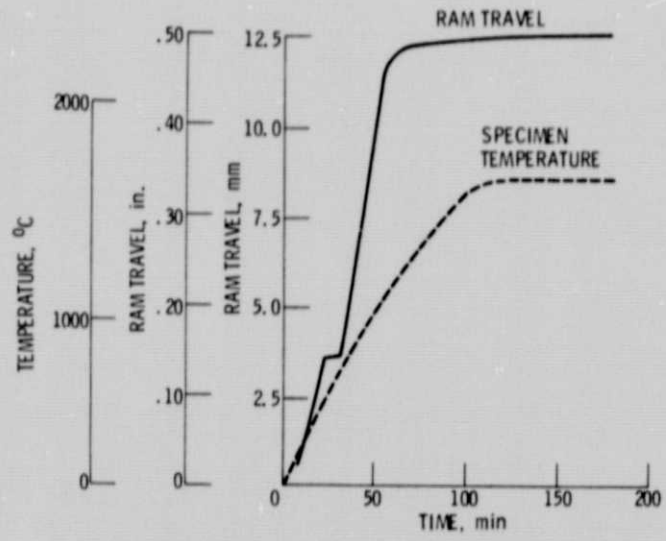
Figure 1. - Hot pressing conditions investigated.



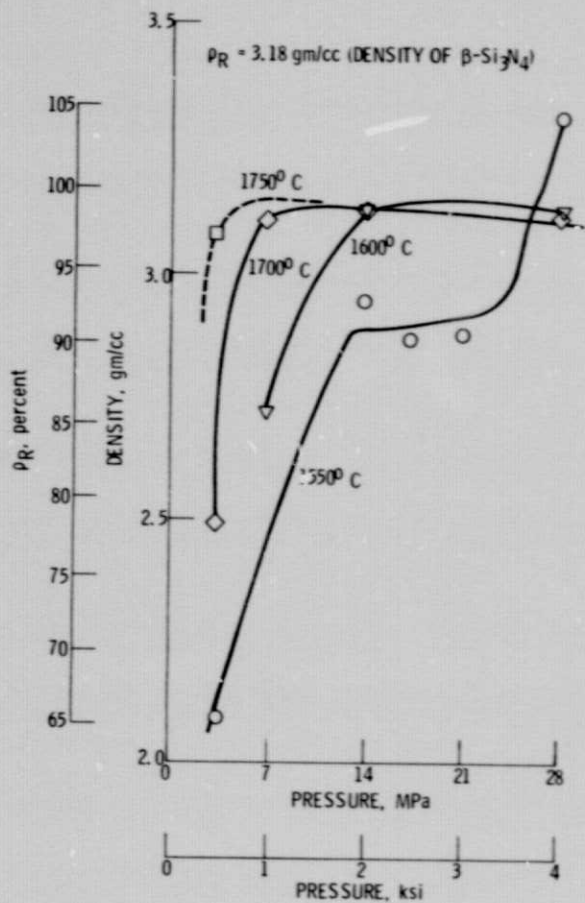Figure 2. - Typical heating rate and ram travel in sialon fabrication at 14 MPa (2 ksi).

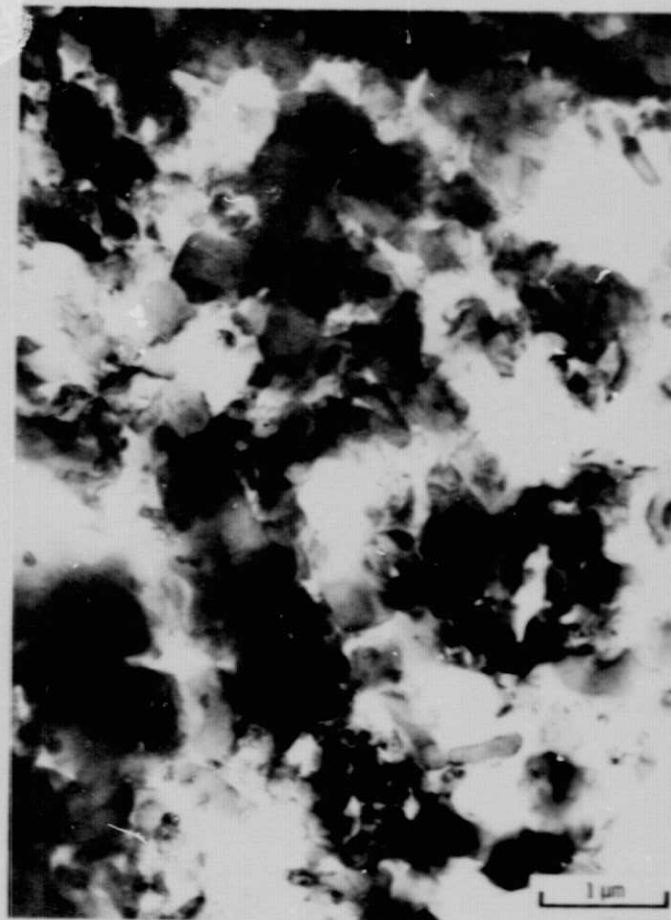Figure 3. - Effect of pressure on density at various temperatures.



Figure 4. - TEM Micrograph of 60 m/o Al₂O₃ - 40 m/o Si₃N₄ compact hot-pressed at 1550° C, 14 MPa (2 ksi) for 2 hours.

Figure 4. - Concluded.

1 μm



.5 μm

Figure 5. - TEM Micrograph of 60 m/o Al$_2$O$_3$ - 40 m/o Si$_3$N$_4$ compact hot-pressed at 1550° C, 27 MPa (4 ksi) for 2 hours.
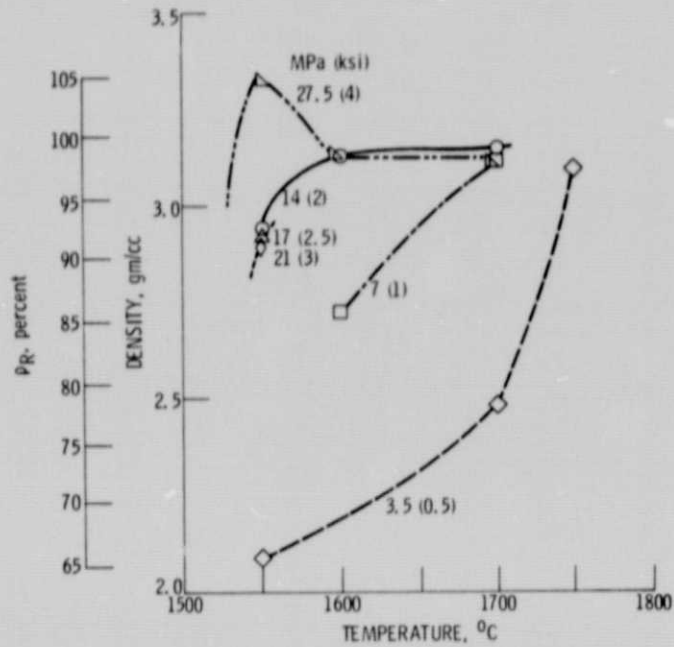
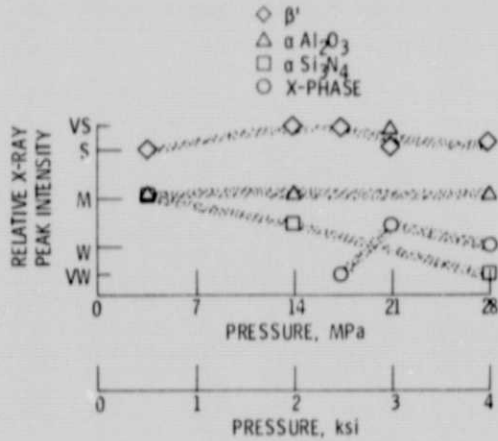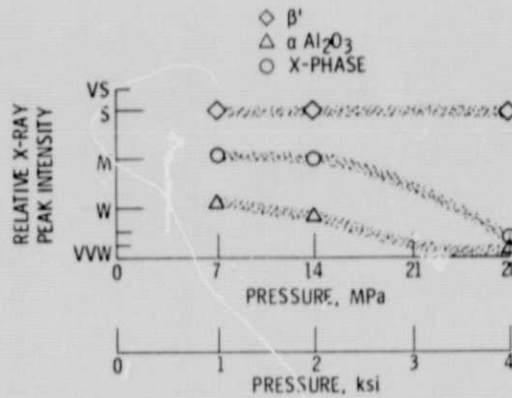Figure 6. - Effect of temperature on density at various pressures.
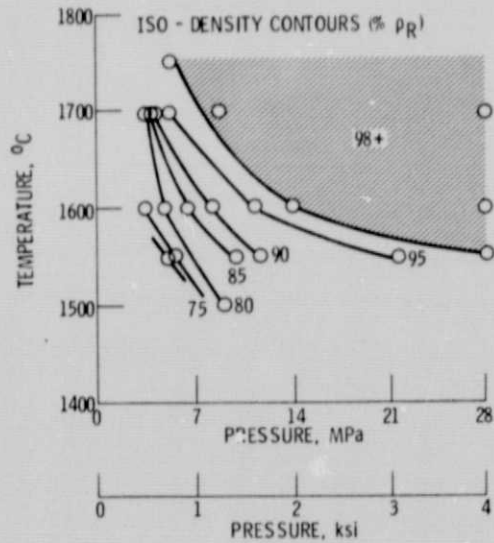


Figure 7. - Iso-density contours (% $\rho_R$) for
60 m/o Al$_2$O$_3$ - 40 m/o Si$_3$N$_4$ powder com-
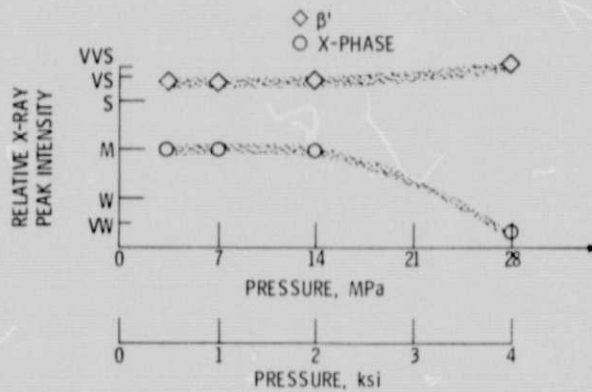pacts hot pressed for 2 hours.

(a) PHASE VARIATION AS A FUNCTION OF
PRESSURE FOR SIALON HOT PRESSED
2 hr AT 1550° C.

Figure 8.



(b) PHASE VARIATION AS A FUNCTION OF
PRESSURE FOR SIALON HOT PRESSED
2 hr AT 1600° C.

Figure 8. - Continued.



(c) PHASE VARIATION AS A FUNCTION OF PRESSURE FOR
SIALON HOT PRESSED 2 hr AT 1700° C.
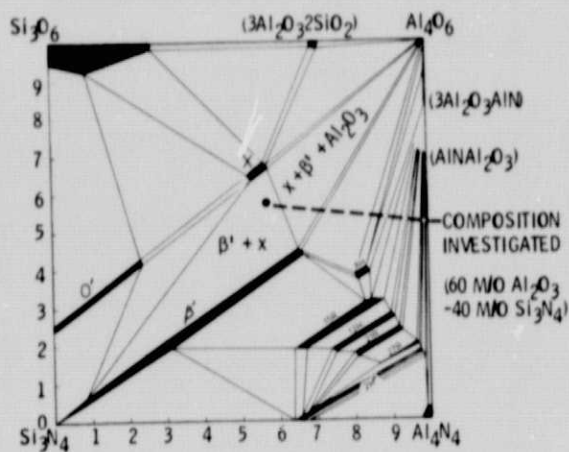
Figure 8. - Concluded.

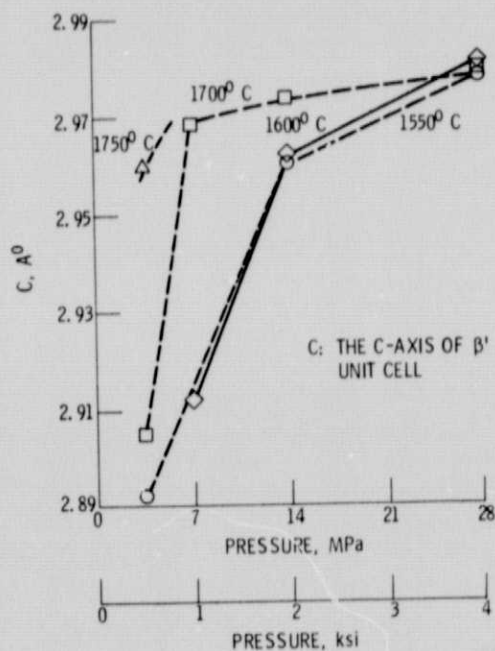Figure 9. - The $Si_3N_4$-AlN-$Al_2O_3$-$SiO_2$ system (from ref. 9).



Figure 10. - Pressure and temperature effects on lattice parameter of $\beta$ phase.

| 1. Report No. NASA TM-78945 | 2. Government Accession No. | 3. Recipient's Catalog No. |
|---|---|---|
| 4. Title and Subtitle EFFECTS OF PRESSURE AND TEMPERATURE ON HOT PRESSING A SIALON | | 5. Report Date |
| | | 6. Performing Organization Code |
| 7. Author(s) Hun C. Yeh and William J. Waters | | 8. Performing Organization Report No. E-9692 |
| 9. Performing Organization Name and Address National Aeronautics and Space Administration Lewis Research Center Cleveland, Ohio 44135 | | 10. Work Unit No. |
| | | 11. Contract or Grant No. |
| 12. Sponsoring Agency Name and Address National Aeronautics and Space Administration Washington, D.C. 20546 | | 13. Type of Report and Period Covered Technical Memorandum |
| | | 14. Sponsoring Agency Code |

15. Supplementary Notes

16. Abstract

Mixed powders (60 m/o $Al_2O_3$-40 m/o $Si_3N_4$) were hot pressed at temperatures and pressures from $1360^{\circ}$ to $1750^{\circ}$ C and 3.5 to 27.5 MPa (0.5 to 4.0 ksi). Fully dense sialon bodies are obtainable at temperatures and pressures as low as $1550^{\circ}$ C and 0.5 ksi. The fully dense bodies contain $\beta'$ and x-phase. There is some evidence that plastic deformation has contributed to densification.

| 17. Key Words (Suggested by Author(s)) Ceramics Sialon Hot pressing | 18. Distribution Statement Unclassified - unlimited STAR Category 27 |
|---|---|

| 19. Security Classif. (of this report) Unclassified | 20. Security Classif. (of this page) Unclassified | 21. No. of Pages | 22. Price* |
|---|---|---|---|